International Journal of Civil Engineering

Geotechnical Engineering

Three dimensional bearing capacity analysis of shallow foundations using discrete element method

A. R. Majidi[1] , **A. A. Mirghasemi**[2,*], **M. Arabshahi**[3]

Received: January 2010, Accepted: December 2011

Abstract

In the current study, an effort is made to determine three dimensional bearing capacity of rectangular foundations using Discrete Element Method. The soil mass is modeled as discrete blocks connected with Winkler springs. Different factors affect the geometry of failure surface. Six independent angles are used to define the failure surface. By trial and error, the optimum shape of failure surface beneath the foundation can be found. The paper includes the derivation of the governing equations for this DEM based formulation in three dimensional state as well as parametric sensitivity analyses and comparison with other methods. Moreover, using the current method, bearing capacity coefficients are presented for various friction angles and foundation aspect ratios.

Keywords: 3 Dimensional; Bearing capacity; Shallow foundations/footings; Discrete element method; Numerical modeling/analysis

1. Introduction

Bearing capacity of foundations has always been one of the most interesting research subjects in geotechnical engineering with numerous published papers and reports. Among these, extensive studies have been made for bearing capacity in two dimensions for infinitely long strip footing which rest on a horizontal or inclined slope surface. In this regard, different methods of analysis are introduced. Randolph et.al [1] summarized some of the theoretical advances made over the last few decades in the treatment of bearing capacity of foundations.

It seems that 2D theoretical approaches have reached to a relatively satisfactory level for ordinary loading and soil conditions. But, real foundations are not infinitely long and their failure mechanism is certainly three dimensional. Therefore, developing analytical estimation of 3D bearing capacity is non-trivial.

Evaluation of the 3D bearing capacity of shallow foundations is usually assessed by introducing experimental and empirical shape factors into the ordinary 2D equations for the strip footings developed by researchers such as Meyerhof [2], Terzaghi and Peck [3], Hansen [4], de Beer [5], Vesic [6], and the others. These empirical shape factors are commonly based on the test results obtained from works of Golder [7] and some additional unpublished data.

Due to differences or even inconsistencies of such proposed experimental and empirical shape factors, these shape factors need to be obtained from a realistic analysis. Therefore, three dimensional problems of bearing capacity still require more experimental and theoretical research activities.

Shield and Drucker [8] presented a theoretical evaluation of 3D bearing capacity of rectangular foundations on homogeneous clay ($\phi = 0$) by means of upper and lower bound solutions. Theoretical analyses of bearing capacity have also made use of Kötter's equation with a rigid perfectly plastic soil response assumption (Shield. [9]; Cox et al., [10]). Nakase [11] used an ordinary limit equilibrium method and assumed cylindrical sliding surfaces for rectangular footings on normally consolidated clays, of which strength increases linearly with depth. Ugai [12] presented more rigorous solutions for rectangular foundations laid on NC clays by means of limit analysis, and also improved the admissible velocity field originally proposed by Shield and Drucker [8], by including the effect of the footing base roughness. Narita and Yamaguchi [13], presented a three dimensional analysis of bearing capacity of rectangular foundations by means of the method of slices, assuming that sliding surfaces are composed

* *Corresponding Author: Aghasemi@ut.ac.ir*
1 Ph.D. of Soil Mechanics and Foundation Engineering, Mahab Ghodss Consulting Engineering Company, Tehran, Iran.
2 Professor, School of Civil Eng., Faculty of Engineering, University of Tehran.
3 Ms.C. of Soil Mechanics and Foundation Engineering, School of Civil Eng., Faculty of Engineering, University of Tehran

of a set of log-spirals with different initial radii in the direction of the longer axis of the footing base. Michalowski [14] introduced a 3D analysis of rectangular foundations based on limit analysis (upper-bound) approach, in which all mechanism of failure considered in the analysis consisted of four regions, each characterized by plane deformations. Then, Michalowski and Dawson [15] compared the results of their proposed upper bound method with the numerical results of FLAC^{3D} code. Also, Zhu and Michalowski [16] calculated shape factors for square and rectangular footings based on the upper bound method they proposed, and compared them with finite element analysis results. Salgado et al. [17] calculated rigorously the bearing capacity of strip, square, circular and rectangular foundations in clay, based on finite element limit analysis.

Among all different methods which investigators have used in their analysis, limit equilibrium and continuum based methods such as finite element and finite differences are the most widely used.

Calculations based on limit equilibrium methods for the problem of bearing capacity, generally do not satisfy all equilibrium conditions; therefore, additional assumptions are required with respect to interslice forces and stresses. Both of the finite element method and the finite difference method require initial stress state of the soil, an appropriate constitutive model for the soil, and proper parameters for the model.

Cundall and Strack [18] established a Discrete Element Method (DEM) to study the micromechanical behaviour of granular materials by modeling assemblies of two dimensional circular particles. In this method each particle is considered as a distinct (discrete) element. The method has been used extensively to model many theoretical and industrial applications using the other different shapes of particles such as polygon (Mirghasemi et al., [19,20]), ellipse (Rothenburg & Bathurst, [21]), spheres (Cundall, [22]), polyhedral (Ghaboussi & Barbosa, [23]) and ellipsoid (Qudefel & Rothenburg, [24]; Ng, [25]).

The new concept of DEM presented here, falls within the framework of the limit equilibrium methodology. In two dimensional state, this method was presented by Chang for analysis of bearing capacity of foundations [26], slope stability [27] and retaining walls [28]. Instead of modeling individual particles, soil mass is treated as a system of blocks connected together by elasto-plastic Winkler springs.

This method is somehow similar to the method which Shi [29] presented for a rock block system called Discontinuous Deformation Analysis (DDA). The method was developed to simulate the failure process and study the mechanism of the rock failure with contact and large displacement in 3D condition.

Considering the compatibility conditions, the boundary stresses on the failure surface and the ultimate bearing capacity of shallow foundations can be obtained. The computed boundary stresses from this method satisfy equilibrium conditions and do not exceed the soil strength. Therefore, additional assumptions are not required with respect to interslice forces and stresses. As Chang stated [26-28], the different loading and soil parameters including weight, surcharge and cohesion, can be simultaneously applied to find the corresponding critical failure surface which offers the minimum bearing capacity. For the analysis, only Young's and shear moduli are additionally required.

In the original DEM used for granular soils, equations are explicitly solved by finite difference method, whereas in the current approach these equations are implicitly solved since the contact between two adjacent blocks always exists.

By developing the concept proposed by Chang [26-28], a three dimensional formulation of the discrete element method is presented in this paper to obtain bearing capacity of rectangular shallow foundations. Also, several examples and graphs are provided to demonstrate the applicability of this method. The computations in this research are carried out using a DEM code written in MATLAB and called BCAP^{3D} (Bearing Capacity Analysis Program in 3 Dimensions).

2. Discrete element model

To determine the three dimensional bearing capacity of rectangular shallow foundations by DEM, it is assumed that three blocks of the soil mass beneath the footing are going to slip in order to define the failure mechanism. The soil mass enclosed in three dimensional space with assumed failure surfaces, is considered as several discrete blocks connected with an infinite number of Winkler springs, as shown in Fig. 1.

Each group of Winkler springs consists of three sets of springs in different orthogonal directions. One set of springs is located in the direction normal to the contact surface to simulate the normal stiffness and the two other sets are placed within the contact surface, perpendicular to each other, to simulate the shear resistance (Fig. 2). Therefore, in comparison with the 2D model, one set of shear spring is added in the contact surface between two adjacent blocks.

The behavior of the normal and shear springs is assumed to be Elasto-Plastic. As shown in Fig. 3, the normal springs do not yield in compression, however in tension, they would yield

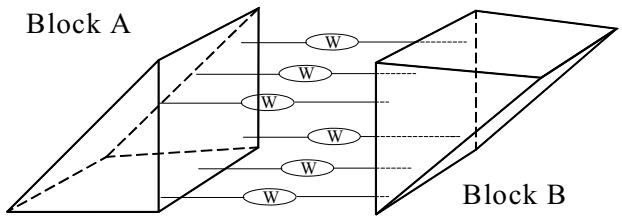

Fig. 1. Connection of adjacent blocks with Winkler springs in 3 dimensional state

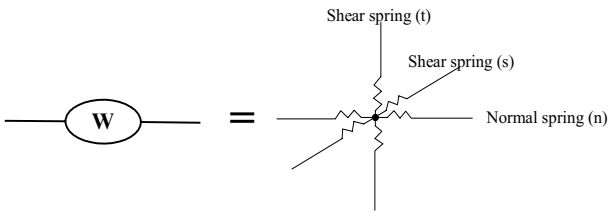

Fig. 2. Winkler spring in 3 dimensional state

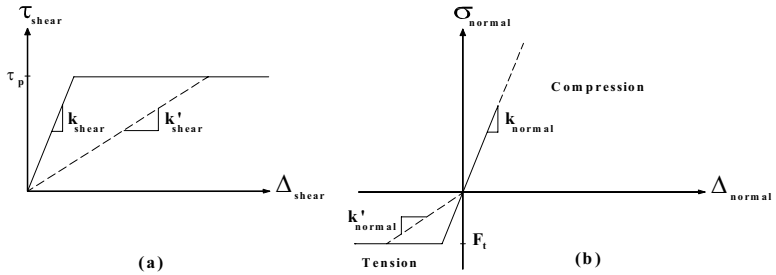

Fig. 3. Stress-Strain behaviour of Winkler springs, (a)- shear springs, (b)- normal springs

at the tensile capacity.

Also, based on Mohr-Coulomb failure criteria, the shear springs yield when the shear strength (τ_p) is reached, as:

$$\tau_p = c + \sigma_n \tan\varphi \quad (1)$$

When stresses in the normal or shear springs exceed their final strength, the springs yield. In order to reduce the stiffness of the yielded springs, a secant method is applied. Regarding the stress-strain relationship shown in Fig. 3, the initial normal stiffness (k_{normal}) alters to reduced secant normal stiffness (k'_{normal}). With the same concept, the initial shear stiffness (k_{shear}) is substituted by the reduced secant normal stiffness (k'_{shear}). The initial values of stiffness in the normal and shear directions between blocks can be estimated using Young's modulus (E) and shear modulus (G), respectively [21-23,26]. This subject will be discussed later in the paper.

3. Failure surface geometry

The model presented here uses some wedges to discretize the assumed failure surface as shown in Fig. 4. Similar to the classical two dimensional bearing capacity approach (Mirghasemi and Majidi, [30]), the failure mechanism contains an active zone blow the footing (zone I), which is pushed downward into the soil mass and a passive wedge (zone III) moves laterally. The transition between downward movement of the active zone and lateral movement of the passive zone takes place through the radial shear zone (II). The shape of the failure surface of zone (II) is assumed to be a logarithmic spiral. These three zones can be divided into any arbitrary number of blocks, e.g. N_1, N_2 and N_3, respectively. The geometry of the failure surface is a function of the footing width (B) and length (L), the internal friction angle of the underlying soil (ϕ) and the six independent angles of α_1, α_2, α_3, α_4, θ_1 and θ_2.

The angles θ_1 and θ_2 as shown in the Fig. 4, determine the inclination of lateral failure surfaces in the three dimensional space. The absolute values of θ_1 and θ_2 are assumed to be identical ($|\theta_1| = |\theta_2|$) due to the symmetry in the foundation geometry and loading. As shown in Fig. 5, a negative or positive value of θ_1 and θ_2 indicates an inwards or outwards inclination of the lateral failure surfaces, respectively. When these angles are zero the lateral failure surfaces are vertical.

Unlike classical methods, these six angles are not predefined

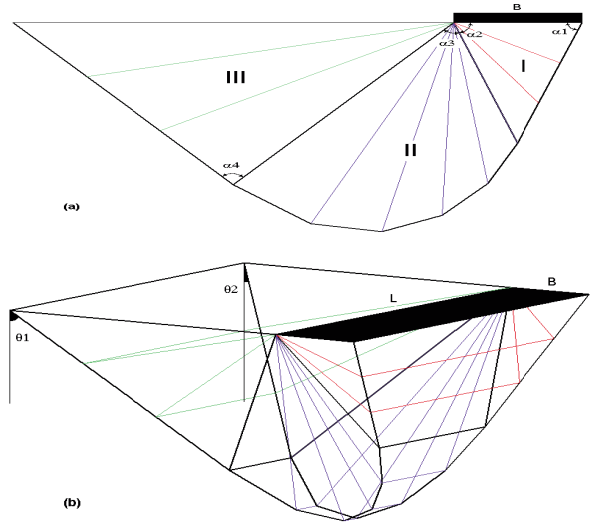

Fig. 4. Aspect of failure surface geometry, (a)- 2D view, (b)- 3D view

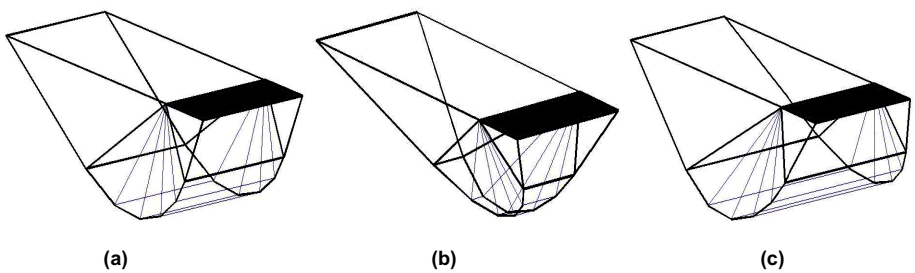

Fig. 5. The inclination of lateral failure surfaces in the three dimensional space, (a)- zero value for θ_1 and θ_2 (vertical), (b)- negative value (inclined inwards), (c)- positive value (inclined outwards).

and are found by iteration to obtain the minimum ultimate bearing capacity. Due to the existence of six independent angles, a very extensive number of failure surfaces are examined to determine the critical failure surface which corresponds to the minimum bearing capacity. Therefore, with more complex failure surface geometry, the accuracy of the solution is improved in comparison with simpler failure surfaces geometry commonly considered in classical limit equilibrium or limit analysis methods.

4. Three dimensional formulation

To obtain a three dimensional formulation of DEM, it is assumed that each block is rigid and only relative displacements of adjacent blocks are taken into consideration. Also in comparison with relative translation, relative rotation of two neighboring blocks is small. Therefore, due to the fact that the two adjacent blocks remain in contact and no separation occurs at contact surfaces under the relative displacement, the continuum theorem can be applied to show the discontinuous deformations in the studied media.

In Fig. 6-a, consider two blocks A and B, which are connected together in (x,y,z) space before displacement. After loading, two contacting blocks are moved and although they exaggeratedly illustrated as separate in Fig. 6-b, they are still in contact, having Winkler springs between them.

Let U_i^A and U_i^B represent the translation and rotation of displacement vector of blocks A and B, respectively (i=1,2,…,6). These vectors in (x,y,z) space contain six components, where three elements (U_1,U_2,U_3) represent translations in (x,y,z) directions and other three elements (U_4,U_5,U_6) represent rotations around these axis. Let point P be the center of the interface surface between these two blocks. The displacement of block B relative to block A at point P is then expressed as follows:

$$\{\Delta P_{x,y,z}\} = [R^b_p]\{U^b\} - [R^a_p]\{U^a\} \quad (2)$$

where $[R_p^a]$ is the matrix joining the centroid of the block A to point P. If, however the block B is fixed, the values of U_i^b are taken as zero. The displacement vector on the left side of Eq. 2 can be transformed from (x,y,z) coordinate to the local (n,s,t) coordinate, which n_i^p is an outward unit vector normal to the side face of block A at point P, as follows:

$$\{\varphi P_{n,s,t}\} = [T]\{\varphi P_{x,y,z}\} \quad (3)$$

where [T] is an orthogonal transformation matrix ($T^T_{ij} = T^{-1}_{ij}$).

Due to the relative translations and rotations between two neighboring blocks, the springs are deformed and the normal and shear stresses are on the interface surfaces can be calculated. Therefore, at any point P' on the interface the springs' deformation in the normal ($\Delta_n P'$) and in shear directions ($\Delta_s P'$,$\Delta_t P'$) can be obtained by:

$$\Delta_n P' = \Delta_n P + \Delta_t w.s_{P'} + \Delta_s w.t_{P'} \quad (4\text{-a})$$

$$\Delta_s P' = \Delta_s P + \Delta_n w.t_{P'} \quad (4\text{-b})$$

$$\Delta_t P' = \Delta_t P + \Delta_n w.s_{P'} \quad (4\text{-c})$$

where ($\Delta_n w$, $\Delta_s w$, $\Delta_t w$) are the relative rotational components of displacement vector in local coordinates. Also, $s_{P'}$ and $t_{P'}$ are the distance of point P' from point P on the interface in s and t directions, respectively. Therefore, the total stress distribution on the interface surface due to relative displacement can be divided as:

(a) Uniform normal stress distribution, due to the relative translation of the centers of the interface surfaces of two adjacent blocks in direction of n axis ($\Delta_n P$).

(b) Triangular normal stress distribution, due to the relative rotation of two adjacent blocks around s axis ($\Delta_s w.t_{P'}$).

(c) Triangular normal stress distribution, due to the relative rotation of two adjacent blocks around t axis ($\Delta_t w.s_{P'}$).

(d) Uniform shear stress distribution, due to the relative translation of two adjacent blocks in the direction of s axis ($\Delta_s P$).

(e) Uniform shear stress distribution, due to the relative translation of two adjacent blocks in the direction of t axis ($\Delta_t P$).

(f) Nonuniform shear stress distribution in the direction of s axis, due to the relative rotation of two adjacent blocks around n axis ($\Delta_n w.t_{P'}$).

(g) Nonuniform shear stress distribution in the direction of t axis, due to the relative rotation of two adjacent blocks around n axis ($\Delta_n w.s_{P'}$).

To obtain the equivalent forces (F_n,F_s,F_t) and moments (M_n,M_s,M_t) in point P, these stresses can be integrated on the

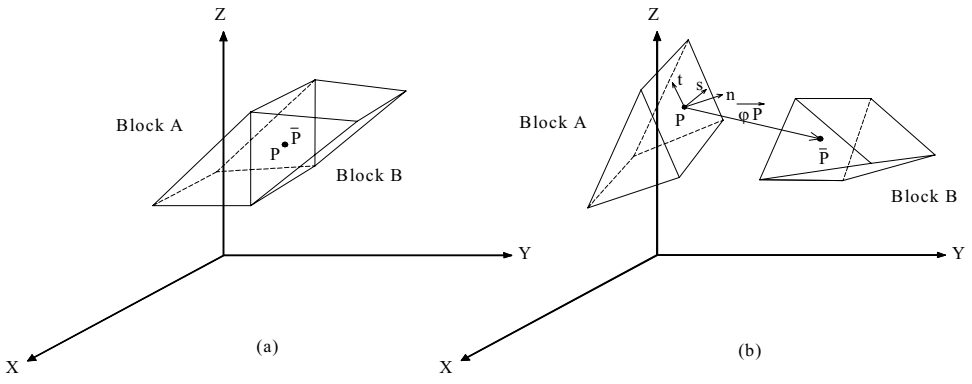

Fig. 6. Displacement of adjacent blocks in 3 dimensional state, (a)- before and (b)- after displacement.

interface surface, as follows:

$$F_n^p = \iint k_n \cdot \Delta_n P \cdot dA + \iint k_n \cdot s_{P'} \cdot \Delta_t w \cdot dA + \iint k_n . t_{P'} \cdot \Delta_s w \cdot dA \quad (5\text{-a})$$

$$F_s^p = \iint k_s \cdot \Delta_s P \cdot dA + \iint k_s . t_{P'} \cdot \Delta_n w \cdot dA \quad (5\text{-b})$$

$$F_t^p = \iint k_t \cdot \Delta_t P \cdot dA + \iint k_t . s_{P'} \cdot \Delta_n w \cdot dA \quad (5\text{-c})$$

$$M_n^p = \iint \left(k_s \cdot \Delta_s P \cdot t_{P'} + k_s \cdot \Delta_n w \cdot t_{P'}^2\right) dA + \iint \left(k_t \cdot \Delta_t P \cdot s_{P'} + k_t \cdot \Delta_n w \cdot s_{P'}^2\right) dA \quad (5\text{-d})$$

$$M_s^p = \iint k_n \cdot \Delta_n P \cdot t_{P'} \cdot dA + \iint k_n \cdot \Delta_t w \cdot s_{P'} \cdot t_{P'} \cdot dA + \iint k_n \cdot \Delta_s w \cdot t_{P'}^2 \cdot dA \quad (5\text{-e})$$

$$M_t^p = \iint k_n \cdot \Delta_n P \cdot s_{P'} . dA + \iint k_n \cdot \Delta_s w \cdot t_{P'} \cdot s_{P'} \cdot dA + \iint k_n \cdot \Delta_t w \cdot s_{P'}^2 \cdot dA \quad (5\text{-f})$$

Where k_n, k_s and k_t are the stiffness coefficients for a unit surface area of normal and shear springs in (n,s,t) directions, respectively.

Since the relative rotation of two adjacent blocks is considered small, it can be assumed that the spring's coefficients k_n, k_s and k_t are constant in Eqs. 5. As a result, similar conditions (elastic or plastic) exist for all springs located at the same direction across the contact surface. The integrals of Eqs. 5 can be obtained from ordinary surface inertial moment equations. Then, Eqs. 5 can be expressed as:

$$\{ F^P_{n,s,t} \} = [k] \{ \Delta P_{n,s,t} \} \quad (6)$$

where [k] is the stiffness matrix of the associated surface. For convenience, the interface forces in the local coordinate are transformed to the global coordinate by:

$$\{ F^P_{x,y,z} \} = [T]^T \{ \Delta F_{n,s,t} \} \quad (7)$$

From Eqs. 2, 3, 6 and 7, the forces acting on all (n) sides of a block should satisfy the force and displacement equilibrium requirement, given by:

$$\{ f^a \} = \sum_{P=1}^{n} -[R^a_p]^T [T^a_p]^T [k^a_p] [T^a_p] [R^b_p] \{U^b\} + [R^a_p]^T [T^a_p]^T [k^a_p] [T^a_p] [R^a_p] \{U^a\} \quad (8)$$

where $\{ f^a \}$ is the body force vector in centroid of block A.

In contrast with finite element method, in which the constraint information is given on nodes, in DEM it is given on the centers of blocks. Based on Eq. 8, the relationship between the forces and the displacements for all blocks can be written as follows:

$$\{f\}=[K]\{U\} \quad (9)$$

where [K] is the global stiffness of system and the vectors { f } and { U } consist of body forces and displacements for all blocks, respectively.

In Eq. 9, there are twelve variables for each block; body forces vector (f^a_x,f^a_y,f^a_z,m^a_x,m^a_y,m^a_z) and displacement vector (u^a_x,u^a_y,u^a_z,w^a_x,w^a_y,w^a_z). Body forces are known, thus the 6N simultaneous equations for a system of N blocks can be solved for 6N unknown variables. The relative displacement of two adjacent blocks can be determined by Eq. 2. The normal and shear forces between blocks can be obtained from Eqs. 3 and 6. Also, the local factor of safety (L.F.S) for each failure surface, and overall factor of safety (O.F.S) for the whole failure surface can be evaluated by the ratio of shear strength force to existing shear force on local and overall failure surface, respectively from:

$$L.F.S = \frac{\tau_p . A}{\sqrt{\left(\tau_s\right)^2 + \left(\tau_t\right)^2} . A} \quad (10\text{-a})$$

$$O.F.S = \frac{\sum \tau_{pi} . A_i}{\sum \sqrt{\left(\tau_{si}\right)^2 + \left(\tau_{ti}\right)^2} . A_i} \quad (10\text{-b})$$

where τ_{si} and τ_{ti} are the existing shear stresses in the directions of s and t on the failure surface. Also, τ_{pi} is the shear strength which can be obtained from Eq. 1.

5. Bearing Capacity Analysis

In this section an example is presented to explain the capability of the method to model the progressive failure in the soil mass under the footings. Also sensitivity analyses are carried out to investigate the effects of various parameters employed in the model.

5.1. Progressive failure modeling

Unlike the limit equilibrium methods, the present method can be used to model progressive failure of a sliding soil mass. In the analysis, an incremental loading procedure is adopted. In each step of the calculations, the load is increased while a linear behaviour is assumed for the Winkler springs. As the load increases, the induced stresses in springs may exceed the allowable stresses. When the shear and normal stresses are beyond the admissible stresses at an interface, the local factor of safety is set to be 1 for the interface and the iteration process redistributes the excessive amount of stresses to the neighboring blocks. The iterative procedure is carried out until the stresses at all interfaces of blocks are compatible with their deformations and completely satisfy the stress-displacement relationships. The Newton-Rophson iterative scheme (Bathe, [31]) is applied for modeling nonlinearity properties in plastic conditions. In this iterative scheme, an approximation to the exact stress-strain curve is made based on the slope at the start of the increment, but using an iterative procedure, in which the stiffness is updated at each iteration, the approximation gets refined.

Fig. 7 shows the geometry of the assumed failure mechanism composed of discrete blocks under a rectangular footing. The unit weight of soil used for this example is 20 kN/m^3, the angle of internal friction of soil is 30° and the soil cohesion is 30 kPa. The values of Young's modulus and shear modulus are assumed to be 3 and 1 MPa, respectively. The footing width and length are B = 1 m and L = 2 m. The number of blocks in zones I, II and III are selected as 1, 5 and 1 respectively (Fig. 4). In classical 2D limit methods [2-4,6], the critical angles related to the minimum bearing capacity, are often obtained by assumption or by derivation and usually fixed at ($\alpha_1 = \alpha_2 = \pi/4 + \phi/2$), ($\alpha_3 = \pi/2$) and ($\alpha_4 = \pi/2 + \phi$). Therefore, in this example the angles α_1 to α_4 are chosen to be 60, 60, 90 and 120 degrees, respectively. Also, the angles θ_1 and θ_2 are assumed zero; it

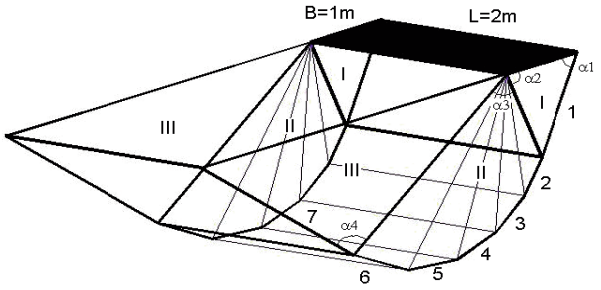

Fig. 7. Discrete element mesh for modeling progressive failure

means that the lateral failure surfaces are vertical. The results of computation are summarized in Table 1 and 2 for base (B_i) and lateral (L_i) failure surfaces. As indicated in Table 1, as the load is incrementally increased, more shear springs along the failure surfaces yield. The reduction of local factor of safety to 1 at each interface indicates that all shear springs of the interface are yielded. As loading increases, the number of plastic interfaces is also increased and the overall factor of safety is reduced. Finally at the ultimate bearing load equal to 5177.95 kN, all interface springs, both in base and lateral surfaces, experience plastic condition and the overall factor of safety of 1 is resulted.

Table 1. Progressive failure in shear springs on base failure surfaces

o 5-)bcd))e)bo und- tio n)a- d)(kN)	500	1000	2000	4000	5177c95
bcd)[B_1]	1c000	1c000	1c000	1c000	1c000
bcd)[B_2]	1cl10	1c000	1c000	1c000	1c000
bcd)[B_3]	1c797	1c032	1c000	1c000	1c000
bcd)[B_4]	3cl21	1c646	1c000	1c000	1c000
bcd)[B_5]	6c599	2c982	1c490	1c000	1c000
bcd)[B_6]	37c919	7c648	2c730	1c223	1c000
bcd)[B_7]	19c623	169c976	6c098	1c717	1c000
Over- a)f- 5to r)o f)s- fety	2c248	1c649	1c255	1c044	1c000

Table 2. Progressive failure in shear springs on lateral failure surfaces

Local F.S | Foundation load (kN)	500	1000	2000	4000	5177.96
F.S [L_1]	1.000	1.000	1.000	1.000	1.000
F.S [L_2]	1.000	1.000	1.000	1.000	1.000
F.S [L_3]	1.360	1.000	1.000	1.000	1.000
F.S [L_4]	2.340	1.167	1.000	1.000	1.000
F.S [L_5]	3.888	2.095	1.000	1.000	1.000
F.S [L_6]	5.024	3.828	1.789	1.000	1.000
F.S [L_7]	5.102	5.715	3.986	1.133	1.000
Overall factor of safety	2.248	1.649	1.255	1.044	1.000

5.2. Influence of the number of blocks

As mentioned previously, the soil mass beneath the footing is divided into several distinct and rigid blocks connected with Winkler springs. The effect of the number of blocks used for each failure zone under the footing is investigated and the results are presented in Table 3. As it can be seen in this table, the number of blocks at three failure regions (N_1, N_2 and N_3) vary in all possible combinations of 1, 5 and 10. Hence, the resultant ultimate bearing capacity is calculated. As it is expected, the best result which corresponds to the minimum bearing capacity, is obtained when the number of blocks is 1 in regions (I) and (III), and is 10 (largest in this series of modeling) at region (II). Therefore, it can be concluded that the radial shear zone (II), must be modeled with an adequate number of blocks to simulate the shear behaviour of this zone. Also, due to the non-shear behaviour of zones (I) and (III), one block would be enough to model these regions.

Fig. 8 describes the influence of the number of blocks in zone (II) on the resultant bearing capacity, when the number of blocks in zones (I) and (III) are equal to 1. As shown, by increasing the number of blocks in zone (II), the ultimate bearing capacity decreases. However, it seems that by modeling this region with block quantities higher than 10, sufficient accuracy is obtained. Thus, in most cases, which will be presented here later, for obtaining enough accuracy, the number of blocks in zones (I), (II) and (III) is chosen to be 1, 25 and 1, respectively.

5.3. Influence of the foundation aspect ratio

In Fig. 9 the influence of the foundation aspect ratio (L/B) on the ultimate bearing capacity in unit area ($q_{Ult.}$) is shown. As expected, the ultimate bearing capacity decreases by increasing the footing aspect ratio. Finally, this value reaches to its 2D ultimate bearing capacity which is obtained in this example equal to 1204.43 kPa.

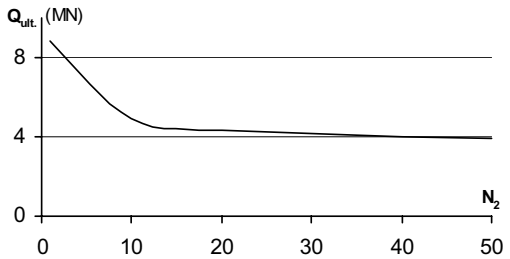

Fig. 8. Influence of the number of blocks in zone II (N_2) on Q_{ult}

Table 3. Influence of number of blocks (N_1,N_2,N_3) in the three failure regions (I,II,III)

N_1: No. of blocks in region (I)	1	1	1	1	1	1	1	1	1	5	5	5	5	5	5	5	5	5	10	10	10	10	10	10	10	10	10
N_2: No. of blocks in region (II)	1	1	1	5	5	5	10	10	10	1	1	1	5	5	5	10	10	10	1	1	1	5	5	5	10	10	10
N_3:No. of blocks in region (III)	1	5	10	1	5	10	1	5	10	1	5	10	1	5	10	1	5	10	1	5	10	1	5	10	1	5	10
$Q_{ult.}$(MN)	8.8	9.2	10.0	5.2	5.6	5.7	4.9	5.3	5.4	5.8	7.3	9.5	5.2	5.7	5.8	5.1	5.5	5.5	5.1	6.5	8.1	5.2	5.6	5.6	5.1	5.4	5.3

5.4. Effect of Winkler spring constant

As indicated previously, the initial values of stiffness in the normal and shear directions between blocks can be estimated by taken analogous to the values of Young's modulus (E) and shear modulus (G), respectively. For isotropic elastic materials, the ratio of (E/G) is given by 2(1+ν), in which (ν) is the Poission's ratio and varies from 0 to 0.5 for different soils. Thus, the practical range of (k_{normal}/k_{shear}) is from 2 to 3. Similar to the 2D model (Chang, [26]), it is found that the results of the present method depend on the Winkler spring constants ratio (k_{normal}/k_{shear}) rather than their individual values. In Fig. 10, the influence of the variation of (k_{normal}/k_{shear}) is described. As the results show, the computed collapsing load is not significantly affected by variation of (k_{normal}/k_{shear}), in the practical range of (E/G) ratio.

6. Two dimensional bearing capacity coefficients

The two dimensional bearing capacity estimation is generally based on the superposition method proposed by Terzaghi [32], in which the contribution of different loading and soil parameters including self-weight (γ), internal friction angle (ϕ), surface surcharge (q) and cohesion (c), are expressed in the form of non-dimensional bearing capacity coefficients as follows:

$$q_{ult.}=0.5B\gamma N_{\gamma}+qN_q+cN_c \quad (11)$$

where N_{γ}, N_q and N_c are the two dimensional bearing capacity coefficients (i.e. self- weight, surcharge and cohesion coefficients).

In classical limit analysis methods, the exact values of surcharge and cohesion bearing capacity coefficients are obtained from:

$$N_q = tg^2(\frac{\pi}{4}+\frac{\varphi}{2}).\exp(\pi tg\varphi) \quad (12)$$

$$N_c = (\frac{N_q - 1}{tg\,\varphi}) \quad (13)$$

by assumption of ($\alpha_1=\alpha_2=\pi/4+\phi/2$), ($\alpha_3=\pi/2$) and ($\alpha_4=\pi/2+\phi$) for angles which define the failure surface geometry in 2D. But, as mentioned previously, there is no special presumption in determination of the failure surface angles in present method.

To compute the cohesion coefficient N_c in DEM, the unit weight of the soil and the load surcharge were set to be zero and c = 9.8 kPa. By assuming γ= 0, c = 0 and q = 9.8 kPa, the N_q can be calculated. On the other hand, assuming c = 0, q = 0 and γ = 19.6 kN/m^3 would results in the N_{γ}. The width of footing (B) and the Winkler spring constant ratio (E / G) were assumed 1 m and 2.7, respectively in all computations. Also, In order to make the 3D DEM results comparable to the 2D available solutions, the footing aspect ratio (L/B) was set to 1000.

In Figs. 11 and 12, the values of N_q and N_c obtained by Eqs. 12 and 13 are compared with the results of DEM which are obtained with assumption of the above mentioned classical failure surface angles and so with critical angles found by trial and error. As it can be seen, the N_q and N_c values obtained from Eqs. 12 and 13 are almost identical to DEM results which are obtained with assumption of classical failure surface angles. However, the critical values of N_q and N_c in DEM are obviously less than classical exact values.

On the other hand, the values of N_{γ} obtained from various methods and the proposed DEM are compared in Fig. 13. From this comparison, it is concluded that the values of N_{γ} obtained by the DEM presented here, are very close to the results of Vesic [6] method. These differences in various methods are not surprising. For instance, forϕ = 40°, N_{γ} varies between 38 to 192 in different 2D methods (Bowles [33]).

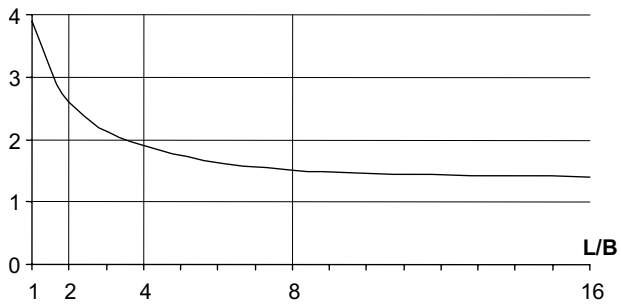

Fig. 9. Influence of the foundation aspect ratio (L/B) on q_{ult}

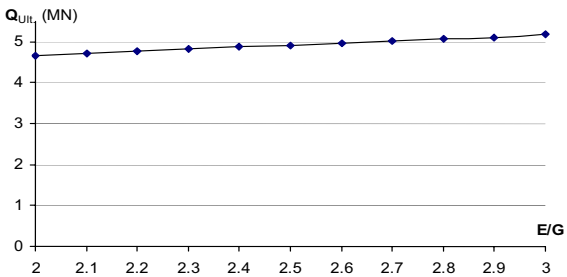

Fig. 10. Influence of variation of the Winkler springs stiffness ratio (k_{normal} / k_{shear}) on Q_{ult}

7. Three dimensional bearing capacity coefficients

3D Bearing capacity estimation is generally based on the superposition method proposed by Terzaghi [32] and expressed in the form of dimensionless bearing capacity coefficients as follows:

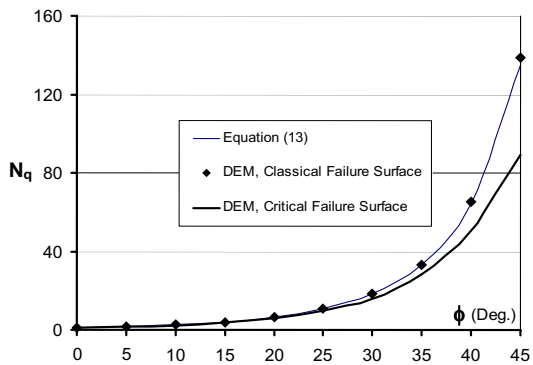

Fig. 11. Comparison of exact mathematical values of N_q and DEM in 2D state

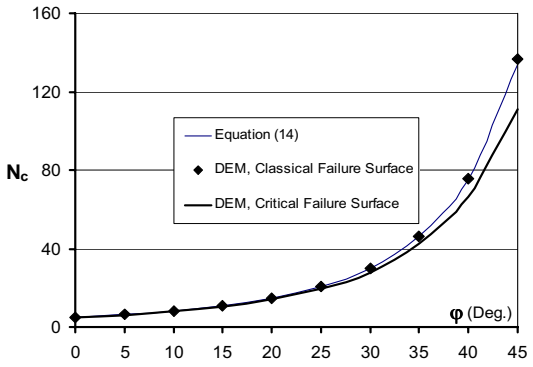

Fig. 12. Comparison of exact mathematical values of N_c and DEM in 2D state

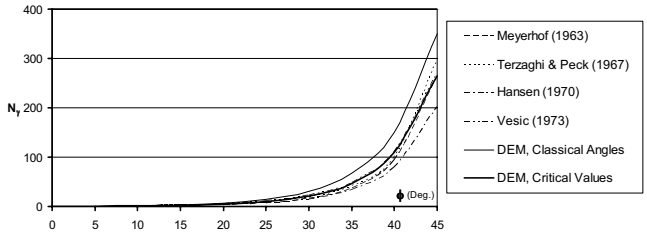

Fig. 13. Comparison of N_γ obtained from conventional methods and DEM in 2D state

$$q_{ult.} = 0.5B\gamma N'_\gamma + qN'_q + cN'_c \quad (14)$$

where three dimensional bearing capacity coefficients (N'_γ, N'_q and N'_c) include the related shape factors (s_γ, s_q, s_c) in the form of:

$$N'_\gamma = s_\gamma . N_\gamma \quad (15\text{-a})$$

$$N'_q = s_q . N_q \quad (15\text{-b})$$

$$N'_c = s_c . N_c \quad (15\text{-c})$$

in which N_γ, N_q and N_c are the ultimate bearing capacity coefficients for a strip footing in 2D.

In this paper, in order to follow the superposition method, the bearing capacity coefficients are calculated and presented here, using DEM. Initially, some comparisons are made with previous published data, then for a practical range of friction angles and footing aspect ratios, the bearing capacity coefficients and related shape factors are provided in several tables and figures.

7.1. Comparison with other 3D methods

To compare the 3D bearing capacity coefficients resulted from DEM with other methods, the results of two classic semi-empirical methods which presented by Meyerhof [2] and Hansen [4] and are widely used for the shape factors, and two latest solutions of 3D bearing capacity of foundations obtained by slices method (Narita and Yamaguchi, [13]) and an upper-bound approach of limit analysis (Michalowski,[14]) are presented in Figs. 14 to 19 for ϕ= 30º and 40º. As can be observed, the differences between the methods increase as the angle of internal friction of the soil increases.

Like almost all other methods evaluating the foundation bearing capacity, the result of the present method is highly dependent on the internal friction of the soil, especially for amounts of ϕ greater than 30º. For large internal friction angles the bearing capacity coefficients and related shape factors are rapidly increasing when the foundation aspect ratio (L/B) approaches to 1, whereas for small internal friction angles the rate of changes is less.

The upper bound method, which was presented by Michalowski [14], offers much higher values especially for small foundation aspect ratios in comparison with other methods. However, at a later point, Michalowski and Dawson [15] compared these results of kinematic approach of limit analysis with the numerical results obtained from FLAC^{3D} code, and indicated that assumptions made in 3D limit analysis provide significant restrictions on the velocity field. Consequently, they concluded that numerical results based on the FLAC^{3D} code provide significantly lower and therefore

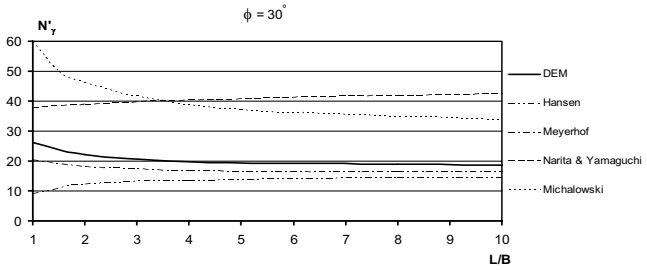

Fig. 14. Comparison of N'_γ obtained from various methods for ϕ= 30º

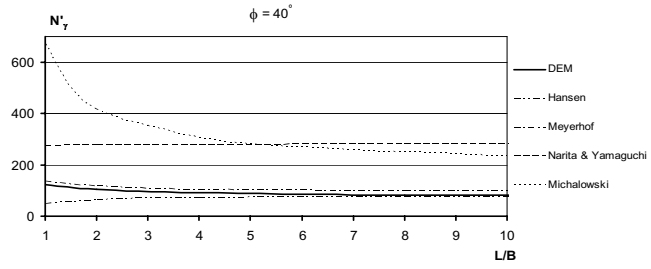

Fig. 15. Comparison of N'_γ obtained from various methods for ϕ= 40º

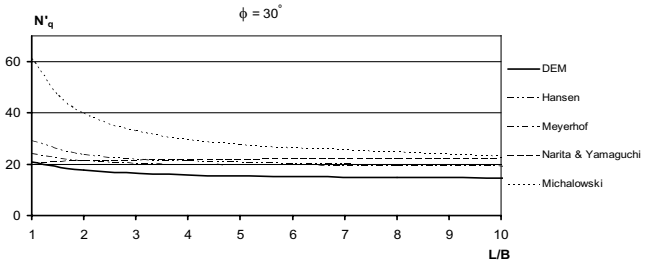

Fig. 16. Comparison of N'_q obtained from various methods for ϕ= 30º

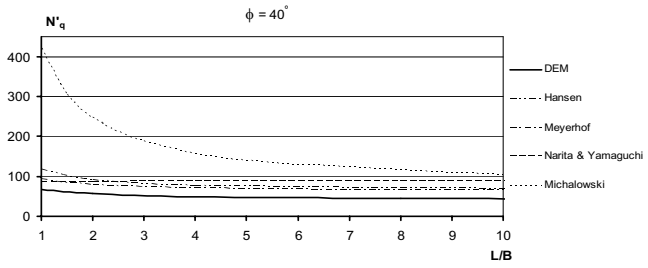

Fig. 17. Comparison of N'_q obtained from various methods for ϕ= 40º

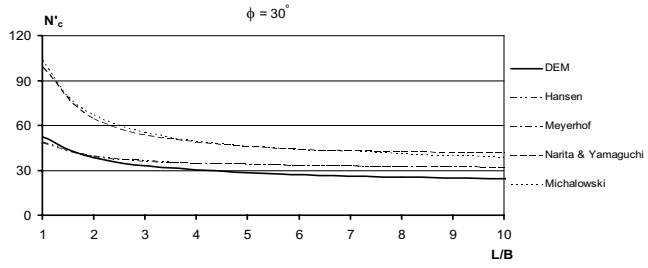

Fig. 18. Comparison of N'_c obtained from various methods for ϕ= 30º

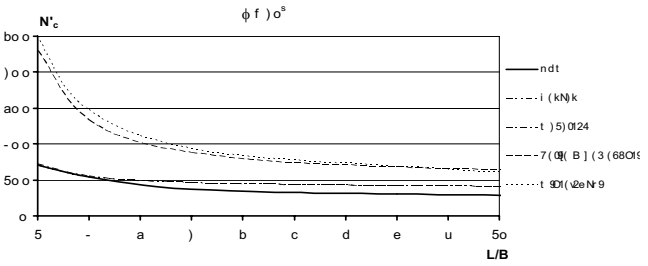

Fig. 19. Comparison of N'_c obtained from various methods for ϕ= 40º

more accurate limit loads.

The result of Narita & Yamaguchi method [13] is different from other classical methods. Due to assumption of a rather simple model for failure surfaces geometry, the elimination of the forces acting on the lateral surfaces and some other assumptions made to satisfy the equilibrium equations, the accuracy of the solution is not satisfactory.

The results of DEM are more in accordance with classical semi-empirical results such as Meyerhof [2] and Hansen [4].

7.2. Superposition method in 3D bearing capacity

The validation of superposition method in the calculation of 3D bearing capacity is examined in Fig. 20. The values obtained using DEM with assumption of Terzaghi's superposition method (Eq. 15) compared with the results of analyses in which the underneath soil possesses different loadings and soil parameters including weight, surcharge and cohesion for ϕ=10 to 40 degrees. The figure shows that the superposition assumption offers conservative results except in small L/B ratios and large amounts of ϕ. For ϕ smaller than 40°, differences between these two approaches do not exceed about 10 percents. Therefore, assuming the Terzaghi type formula of bearing capacity still holds good results for 3D problems.

7.3. Three dimensional bearing capacity coefficients and shape factors

In Tables 4 to 6, the Values of 3D bearing capacity coefficients for various internal friction angles and footing aspect ratios (L/B), obtained by DEM are presented. Also, the values of related shape factors (Eqs. 12), obtained from these tables, are presented in Figs. 21 to 23.

8. Summary and conclusions

In this research, analyses based on Discrete Element Method (DEM) are carried out for determining three dimensional bearing capacity of shallow foundations. The soil mass in the assumed three dimensional failure surface is considered as several discrete blocks connected with Winkler springs. Using an iterative method, the six angles defining the failure surface geometry are independently varied in order to obtain the most critical failure mechanism corresponding to the minimum bearing capacity. The derivation of the three dimensional DEM formulation is explained and several examples expressing the progressive failure and sensitivity analysis are provided. The results are compared with other 2D and 3D

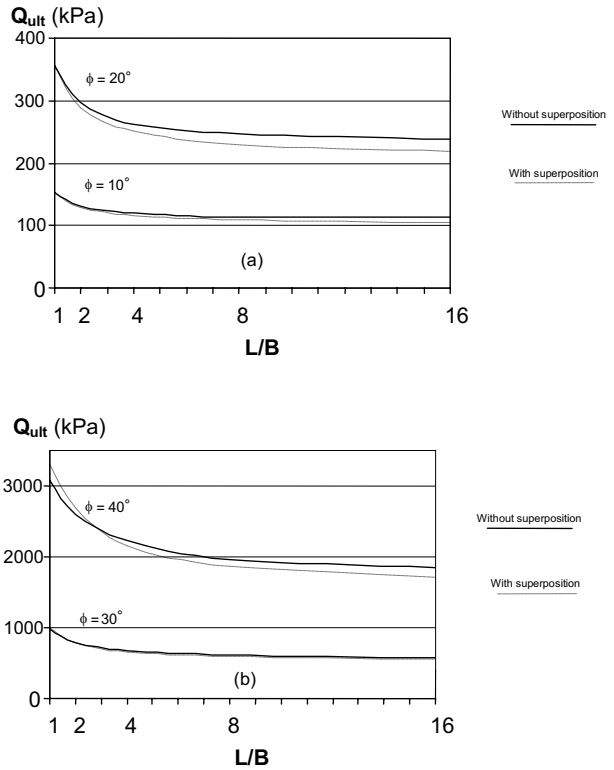

Fig. 20. Investigation of superposition method on bearing capacity in 3 dimensional conditions,
(a)- for ϕ= 10° and 20°, (b)- for ϕ= 30° and 40°

Table 4. Values of N'_{γ} for various angles of internal friction and footing aspect ratios

ϕ (Deg.)	0°	5°	10°	15°	20°	25°	30°	35°	40°	45°
L/B = 1	0.00	0.35	1.15	2.66	5.83	12.63	26.28	56.19	122.98	273.19
L/B = 2	0.00	0.31	1.01	2.44	5.01	10.67	22.20	47.56	104.14	224.49
L/B = 4	0.00	0.28	0.96	2.30	4.68	9.50	19.61	40.86	91.08	204.80
L/B = 8	0.00	0.27	0.92	2.18	4.43	9.10	18.81	38.94	82.34	181.06
L/B=16	0.00	0.26	0.91	2.13	4.28	8.72	17.93	37.36	80.15	163.49
2 Dim.	0.00	0.25	0.87	2.10	4.20	8.51	17.31	35.55	74.65	147.78

Table 5. Values of N'_{q} for various angles of internal friction and footing aspect ratios

ϕ (Deg.)	0°	5°	10°	15°	20°	25°	30°	35°	40°	45°
L/B = 1	1.00	1.72	2.70	4.14	6.95	11.65	20.67	37.20	67.08	125.05
L/B = 2	1.00	1.62	2.49	3.80	6.25	10.34	17.69	31.36	56.63	106.27
L/B = 4	1.00	1.56	2.36	3.59	5.74	9.39	15.75	27.21	49.19	94.83
L/B = 8	1.00	1.54	2.28	3.48	5.48	8.88	14.78	24.90	43.91	83.36
L/B=16	1.00	1.53	2.24	3.39	5.30	8.53	14.31	23.28	41.09	73.89
2 Dim.	1.00	1.52	2.19	3.30	5.16	8.27	13.54	21.99	37.82	66.54

Table 6. Values of N'_{c} for various angles of internal friction and footing aspect ratios

ϕ (Deg.)	0°	5°	10°	15°	20°	25°	30°	35°	40°	45°
L/B = 1	6.52	8.50	11.47	15.85	22.86	34.78	52.34	83.60	141.14	248.81
L/B = 2	5.60	7.17	9.36	12.58	17.61	25.69	38.33	61.82	107.63	205.24
L/B = 4	5.12	6.46	8.27	10.79	14.67	20.57	30.04	45.88	75.04	135.44
L/B = 8	4.86	6.02	7.62	9.97	13.06	18.08	25.25	38.59	60.30	99.26
L/B=16	4.69	5.84	7.32	9.41	12.27	16.82	22.94	34.45	50.46	83.34
2 Dim.	4.54	5.60	7.01	8.90	11.50	15.12	20.66	29.95	42.71	64.46

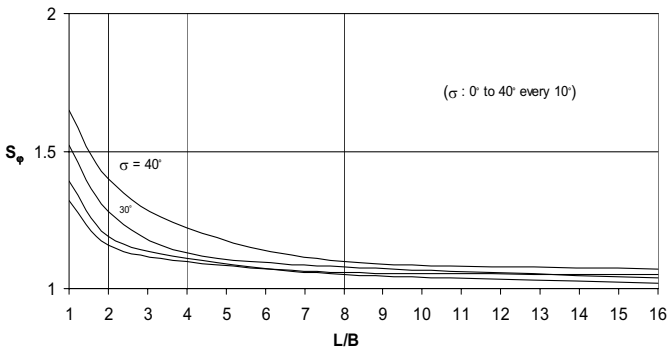

Fig. 21. Self-weight shape factors (s_{γ}) for various ϕ and L/B

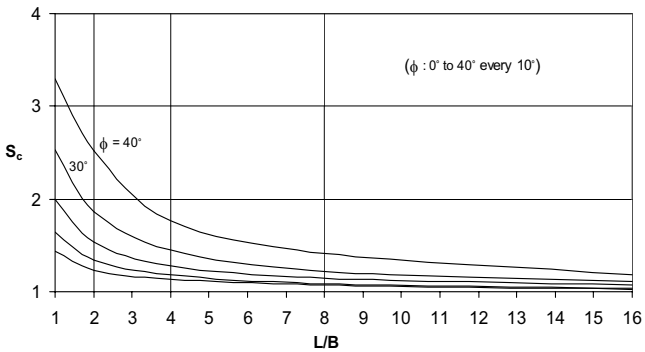

Fig. 23. Cohesion shape factors (s_c) for various f and L/B

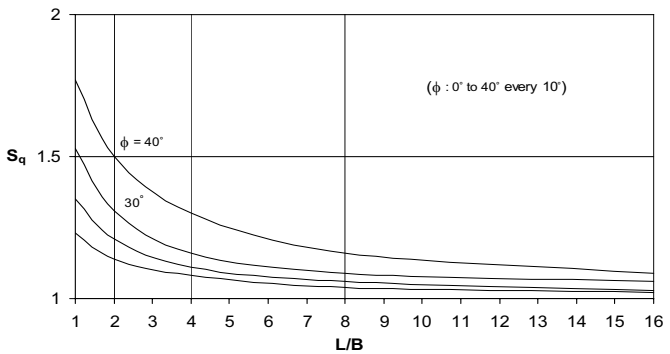

Fig. 22. Surcharge shape factors (s_q) for various f and L/B

bearing capacity analysis. Also the DEM bearing capacity coefficients and related shape factors for various internal friction angles and footing aspect ratios are presented.

The results obtained from the present study can be summarized as follows:

1. DEM can be used to monitor the progressive failure of a sliding soil mass.

2. In DEM, the computed bearing capacity load is not significantly influenced by the ratio of tangential and shear springs (k_{normal} / k_{shear}) in the practical range of (E/G) ratio.

3. The result of DEM analysis with classical failure surface geometry is equal to the classic 2D limit analysis.

However, when the critical surface geometry is found by variation of angles describing the geometry (trial and error), less values for bearing capacity coefficients are obtained.

4. Just like other methods, the bearing capacity coefficients obtained by DEM are highly dependent on the internal friction of the soil, especially for values greater than 30º.

5. For large internal friction angles the bearing capacity coefficients or related shape factors are rapidly increasing when the foundation aspect ratio (L/B) approaches to 1, whereas for small internal friction angles the rate of changes is smaller.

6. The present method results are more in accordance with classical semi-empirical results proposed by earlier researchers such as Meyerhof and Hansen.

7. Self-weight shape factors (s_γ) decreases with increase of L/B ratio.

8. Surcharge (s_q) and cohesion (s_c) shape factors increase with increasing ϕ and decrease with increasing L/B ratio.

9. The superposition assumption offers conservative results except in small L/B ratio and large ϕ. The differences between two approaches (with and without superposition assumption) do not exceed about 10 percents in ϕ amounts smaller than 40°.

References

[1] Randolph, M.F., Jamiolkowski, M,B. and Zdravkovic, L., 2004, "Load carrying capacity of foundations." Advances in geotechnical Engineering: The Skempton Conference, Thomas Telford, London.

[2] Meyerhof, G. G., 1963, "Some Recent Research on the Bearing Capacity of Foundations." In: Canadian Geotech. J., Vol. 1, No. 1, pp. 16-26.

[3] Terzaghi, K. and Peck, R. B., 1967, "Soils Mechanics in Engineering Practice," J.Wiley, New York.

[4] Hansen, J.B., 1970, "A Revised and Extended Formula for Bearing Capacity." Danish Geotech. Inst. Bulletin, No. 28, Denmark.

[5] De Beer, E.E., 1970, "Experimental determination of shape factors and the bearing capacity factors of sands," Géotechnique, Vol. 20, No. 4, pp.387-411.

[6] Vesic, A.S., 1973, "Analysis of Ultimate Loads of Shallow Foundations." J. of Soil Mech. and Fndn Div. ASCE; Vol. 99, No. SM1, pp.45-73.

[7] Golder, H.Q., 1941, "The ultimate bearing pressure of rectangular footings." J. Instn Civ. Engrs., Vol. 17, No. 2, pp.161-174.

[8] Shield, R.T. and Drucker, D.C., 1953, "The application of limit analysis to punch-indentation problems." J. of Appl. Mech., ASCE, pp.453-460.

[9] Shield, R.T., 1955, "On the plastic flow of metals under conditions of axial symmetry." Proc. Roy. Soc. of London A, 233, pp. 267-287.

[10] Cox, A.D., Eason, G. and Hopkins, H.G., 1961, "Axially symmetric plastic deformations in soils." Phil. Trans. Roy. Soc. of London A,Vol. 254, No, 1036, pp. 1-45.

[11] Nakase, A., 1981, "Bearing capacity of rectangular footings on clays of strength increasing linearly with depth." Soils and Foundations, Vol. 21, No. 4, pp. 101-108.

[12] Ugai, K., 1985, "Bearing capacity of square and rectangular footings on nonhomogeneous clays." J. of JSSMFE, Vol. 25, o. 4, pp. 179-185.

[13] Narita, K., Yamaguchi, H., 1992, "Three-dimensional bearing capacity analysis of foundations by use of a method of slices." Soils and Foundations, Vol. 32, No. 4, pp. 143-155.

[14] Michalowski, R.L., 2001, "Upper-bound load estimates on square and rectangular footings." Géotechnique, Vol. 51, No. 9, pp.787-798.

[15] Michalowski, R.L. and Dawson, E.M., 2002, "Three-dimensional analysis of limit loads on Mohr-Coulomb soil." Fndn of Civ. and Inv. Eng., No. 1, pp. 137-147.

[16] Zhu, M. and Michalowski, R.L., 2005, "Shape Factors for Limit Loads on Square and Rectangular footings." J. of Geotech. and Geoenv. Eng. ASCE, Vol. 131, No. 2, pp. 223-231.

[17] Salgado, R., Lyamin, A.V., Sloan, S.W. and Yu, H.S., 2004, "Two- and three-dimensional bearing capacity of foundations in clay." Géotechniqu, Vol. 54, No. 5, pp. 297-306.

[18] Cundall, P.A. and Strack, O.D.L., 1979, "A discrete numerical model for granular assemblies." Géotechnique, Vol. 29, No. 1, pp. 47-56.

[19] Mirghasemi, A.A., Rothenburg. L. and Matyas, E.L., 1997, "Numerical simulations of assemblies of two-dimensional polygon-shaped particles and effects of confining pressure on shear strength." Soils and Foundations, Vol. 37, No. 3, pp. 43-52.

[20] Mirghasemi, A.A., Rothenburg, L. and Matyas, E.L., 2002, "Influence of particle shape on engineering properties of assemblies of two-dimensional polygon-shaped particles." Géotechnique, Vol. 52, No. 3, pp. 209-217.

[21] Rothenberg, L., Bathurst, R.J., 1992, "Micromechanical features of granular assemblies with planner elliptical particles." Géotechnique, Vol. 42, No. 1, pp. 79-95.

[22] Cundall, P.A., 1988, "Computer Simulations of Dense Sphere Assemblies." In: M. Satake, J.T. Jekins, (ed.), Micromechanics of Granular Materials, pp. 113-123, Amsterdam, Netherland.

[23] Ghaboussi, J. and Barbosa, R., 1990, "Three-dimensional discrete element method for granular materials." Int. J. for Numerical and Analytical Methods in Geomechanics, Vol. 14, pp. 451-472.

[24] Qudefel, H. and Rothenburg, L., 1999, "Algorithm for detecting inter-ellipsoid contacts." Comput. and Geotech. Vol. 24, pp. 245-263.

[25] Ng, T.T., 2004, "Shear strength of assemblies of ellipsoidal particles." Géotechnique, Vol. 54, No. 10, pp. 659-669.

[26] Chang, C.S., 1991, "Discrete element method for bearing capacity analysis." Comput. and Geotech., Vol. 12, pp. 273-288.

[27] Chang, C.S., 1992, "Discrete element method for slope stability analysis." J. of Geotech. Engng., Vol. 118, No. 12, pp.1889-1905.

[28] Chang, C.S., 1994, "Discrete element analysis for active and passive pressure distribution on retaining wall." Compu. and Geotech., Vol. 16, pp. 291-310.

[29] Shi, G.H., 2001, "Three dimensional discontinuous deformation analysis." Proc. of the 38th US Rock Mechanics Symposium, Washington D.C., pp. 1421-1428.

[30] Mirghasemi, A.A. and Majidi, A.R., 2002, "Static and pseudo-static bearing capacity analysis of shallow foundations by discrete element method." Proc. of 5th European Conf. of Num. Meth. in Geotech. Engng, Paris, pp. 337-342.

[31] Bathe, K.J., 1982, "Finite element procedures in engineering analysis." Prentice-Hill, Englewood Cliffs, New Jersey.

[32] Terzaghi, K., 1943, "Theoretical soil mechanics." J. Wiley, New York.

[33] Bowles, J.E., 1996, "Foundation analysis and design." 5th edition, McGraw-Hill, New York.